Luminescence Quenching of Dyes by Oxygen in Core−Shell Soft-Sphere Ionic Liquids

Bao-Hang Han and Mitchell A. Winnik*

Department of Chemistry, University of Toronto, 80 St. George Street, Toronto, Ontario M5S 3H6, Canada

Athanasios B. Bourlinos and Emmanuel P. Giannelis*

Department of Materials Science and Engineering, Cornell University, Ithaca, New York 14853

Received March 11, 2005. Revised Manuscript Received May 12, 2005

We examined the photoluminescence and susceptibility to quenching by atmospheric oxygen of a series of phosphorescent dyes dissolved in a core−shell "soft-sphere" ionic liquid matrix consisting of a 7 nm diameter silica core surrounded by a mobile phase consisting of end-grafted flexible chains. While this medium is macroscopically uniform in composition, it is locally heterogeneous on the nanometer length scale. Luminescent dyes provide an opportunity for assessing some of the properties of this local heterogeneity. The PL decay profiles of both platinum ocatethyl porphine (PtOEP) and $[Ru(dpp)_3]Cl_2$ could be fitted to a simple exponential form over a range of partial oxygen pressures. Taking the behavior of PtOEP as "normal," we calculate an oxygen permeability in the liquid of $P_{O_2} = 4 \times 10^{-12}$ mol cm^{-1} s^{-1} atm^{-1}, comparable to that of poly(*n*-butyl thionylphosphazene) (C_4PATP) but smaller than that ($18 \pm 2 \times 10^{-12}$ mol cm^{-1} s^{-1} atm^{-1} for poly(dimethylsiloxane) (PDMS). The smaller slope of the Stern−Volmer quenching plot for $[Ru(dpp)_3]Cl_2$ could be rationalized in terms of two factors, the known smaller cross section for quenching by oxygen for this dye coupled with the likelihood that this dye is located in a more rigid ionic environment characterized by a somewhat smaller local diffusion coefficent for oxygen.

Introduction

In this paper we describe photoluminescence (PL) quenching experiments for a series of dyes dissolved in a novel type of ionic liquid,[1,2] which we refer to as a soft-sphere fluid. This concept for this type of liquid is based on the idea of an inorganic nanoparticle bearing a corona of flexible chains.[3] The flexible chains deform to fill the space between the dense hard-core particles and impart fluidity to the system. The ionic nature of the fluid phase derives from the fact that the flexible chains, each bearing an ionic end group, are attached to the core via ion-pair interactions. Since the bulk phase is formed by a close-packed array of these core−shell structures, we find it useful to refer to the system as a core−shell soft-sphere fluid. In this way we recognize the analogy as well as the contrast with hard-sphere fluids such as liquid argon.

Among the many features that make these fluids unique is the nature of their structure on different length scales. While they are macroscopically uniform in composition, typically 10−20% of the volume is occupied by dense inorganic nanoparticles, and this fraction of the volume is not accessible to solutes in the system. On the length scale of the spaces between the dense cores, one expects to find ionic and nonionic domains. A solute in the system might experience a range of different microenvironments or might partition selectively into a subset of these microenvironments.

In this paper we are interested in an ionic liquid fabricated from 7 nm silica nanospheres. The surface is functionalized with a short spacer (see Chart 1) to which an *N*,*N*-didecyl-*N*-methylammonium group is attached. The counterion is an alkylethoxylated sulfate in which the alkyl groups are a mixture of linear $C_{13}H_{27}$- and $C_{15}H_{31}$- chains. The synthesis

* To whom correspondence should be addressed. E-mail: mwinnik@chem.utoronto.ca (M.A.W.); epg2@cornell.edu (E.P.G.).

(1) For reviews on the topic of ionic liquid, see (a) Welton, T. *Chem. Rev.* **1999**, *99* (8), 2071−2083. (b) Wasserscheid, P.; Keim, W. *Angew. Chem., Int. Ed.* **2000**, *39* (21), 3772−3789; *Angew. Chem.* **2000**, *112* (21), 3926−3945. (c) Dupont, J.; de Souza, R. F.; Suarez, P. A. Z. *Chem. Rev.* **2002**, *102* (10), 3667−3692. (d) Rogers, R. D.; Seddon, K. R. *Science* **2003**, *302*, 792−793. (e) Seddon, K. R. *Nature Mater.* **2003**, *2* (6), 363−365. (f) Blanchard, L. A.; Hancu, D.; Beckman, E. J.; Brennecke, J. F. *Nature* **1999**, *399*, 28−29. (g) Sheldon, R. *Chem. Commun.* **2001**, (23), 2399−2407. (h) Davis, J. H., Jr.; Fox, P. A. *Chem. Commun.* **2003**, (11), 1209−1212.

(2) For applications of ionic liquids, see (a) Antonietti, M.; Kuang, D.; Smarsly, B.; Zhou, Y. *Angew. Chem., Int. Ed.* **2004**, *43* (38), 4988−4992. *Angew. Chem.* **2004**, *116* (38), 5096−5100. (b) Kuang, D.; Brezesinski, T.; Smarsly, B. *J. Am. Chem. Soc.* **2004**, *126* (34), 10534−10535. (c) Zhou, Y.; Antonietti, M. *J. Am. Chem. Soc.* **2003**, *125* (49), 14960−14961. (d) Zhou, Y.; Antonietti, M. *Adv. Mater.* **2003**, *15* (17), 1452−1455. (e) Zhou, Y.; Antonietti, M. *Chem. Commun.* **2003**, (20), 2564−2565. (f) Cooper, E. R.; Andrews, C. D.; Wheatley, P. S.; Webb, P. B.; Wormald, P.; Morris, R. E. *Nature* **2004**, *430*, 1012−1016. (g) Itoh, H.; Naka, K.; Chujo, Y. *J. Am. Chem. Soc.* **2004**, *126* (10), 3026−3027. (h) Huang, J.; Jiang, T.; Gao, H.; Han, B.; Liu, Z.; Wu, W.; Chang, Y.; Zhao, G. *Angew. Chem., Int. Ed.* **2004**, *43* (11), 1397−1399; *Angew. Chem.* **2004**, *116* (11), 1421−1423. (i) Taubert, A. *Angew. Chem., Int. Ed.* **2004**, *43* (40), 5380−5382; *Angew. Chem.* **2004**, *116* (40), 5494−5496. (j) Vijayaraghavan, R.; Surianarayanan, M.; MacFarlane, D. R. *Angew. Chem., Int. Ed.* **2004**, *43* (40), 5363−5366; *Angew. Chem.* **2004**, *116* (40), 5477−5480.

(3) Bourlinos, A. B.; Raman, K.; Herrera, R.; Zhang, Q.; Archer, L. A.; Giannelis, E. P. *J. Am. Chem. Soc.* **2004**, *126* (47), 15358−15359.

10.1021/cm050553e CCC: $30.25
Published on Web 06/18/2005

Chart 1. Schematic Structure of Silica Nanoparticle Based Ionic Liquid

and characterization of this material, as well as its viscoelastic properties, are reported elsewhere.[4] The total organic content of the system is 75 wt %, corresponding to ca. 88 vol %. Thus ca. 12% of the volume of the liquid is excluded to the dyes and quenchers we dissolve in this system.

In a luminescence quenching experiment, one examines how the presence of a quencher leads to a decrease in the PL intensity and PL decay rate for dyes dissolved in the sample. For fluid systems, quenching normally involves diffusive collisions of the excited dye and quencher, and the rate constant for quenching is proportional to the dye-quencher mutual diffusion coefficient in the system. When the dye is a large molecule and the quencher is oxygen, the oxygen diffusivity is so much larger than that of the dye that quenching is dominated by oxygen diffusion. For simple liquids, both the dyes and the quenchers are distributed uniformly in the system. Concentration is a well-defined quantity, and diffusion follows Fick's laws. Because of rapid reorientation of solvent molecules and fast relaxation of density fluctuations, dye molecules as solutes experience a uniform environment on the time scale of their excited state lifetimes. In the ionic fluid described above, some of these concepts may not apply. Both dyes and quenchers may partition into different microdomains, leading to nonuniform local concentrations. The hard cores not only exclude volume from the solutes but also act as obstacles to diffusion. As a consequence, these types of experiments can provide interesting information about local features of the structure and dynamics of these core−shell ionic liquids.

We use this ionic fluid as a solvent to dissolve a series of transition metal complex dyes that undergo phosphorescence at ambient temperature in the absence of air or oxygen. From the spectroscopic properties of the dyes in the medium, we obtain some information about their local environment. By carrying out a careful series of measurements on the influence of the partial pressure of oxygen on the PL intensity and luminescence decay rate of the dyes in these solutions, we learn about the oxygen permeability P_{O_2} of the fluid, and we learn about the relative susceptibility of the various dyes to oxygen quenching in this medium. To help interpret these results, we compare them with the results of quenching experiments for these dyes dissolved in two different types of polymer films, both characterized by a low glass transition temperature and high local mobility. Poly(dimethylsiloxane) (PDMS) is a nonpolar medium, whereas poly(*N*-butylthionyl phosphazene) (C_4PATP) is a polar aprotic medium that is able to dissolve both ionic and neutral dyes.

Experimental Section

UV/Vis absorption spectra were obtained using a Lambda 25 UV/Vis Spectrometer (PerkinElmer Instruments) with a conventional 1 × 1 cm quartz cuvette for solution samples. Luminescence spectra and intensities were obtained with a SPEX Industries Inc. Fluorolog II Model SPEX1680 spectrometer. Luminescence decay profiles were obtained with a home-built device using the third harmonic (355 nm) of a pulsed Nd:YAG laser (Spectra-Physics GCR-170) as the excitation source. The laser beam intensity was severely attenuated through a High-Energy Variable Attenuator (Newport, Model 935-10) to prevent sample damage and/or dye photobleaching. A filter BP300-400 was placed in the excitation beam path before the film sample and the emission was passed through another appropriate filter CO470 placed before the detector in order to eliminate scattered excitation light and visible light. The signal was detected by a Hammamatsu 956 photomultiplier tube connected to a Tektronix model 1912 transient digitizer. The decay trace was then digitalized and transferred to a computer for data processing.

Materials. The dyes 2,3,7,8,12,13,17,18-octaethyl-21H,23H-porphine platinum(II) (platinum(II) octaethylporphine; PtOEP), platinum(II) *meso*-tetraphenylporphine (PtTPP), and platinum *meso*-tetrakis(pentafluorophenyl)porphine (PtTFPP) were purchased from Porphyrin Products, Frontier Scientific Inc. (Logan, UT). All the above dyes were used without further purification. Tris(4,7-diphenyl-1,10- phenanthroline)ruthenium(II) chloride (dichlorotris-(4,7-diphenyl-1,10- phenanthroline)ruthenium(II), $[Ru(dpp)_3]Cl_2$) was synthesized in Prof. Manners' group as previously described.[5] Pyrene (99+%) was purchased from Aldrich.

Tetrahydrofuran (THF, 99+%), chloroform ($CHCl_3$, 99.8%), 1,1,1-trichloroethane (TCE, 99+%), and methanol (99%) were obtained from Aldrich. Deionized water (>10 MΩ cm) was obtained through the treatment of distilled water by the MilliQ Water System. Oxygen (Research Grade 4.7, 99.997%) and compressed dry air (impurity H_2O 10 ppm) were obtained from BOC gas. Poly(dimethylsiloxane)methyl-terminated (PDMS, gellike solid, M_w > 500 000, viscosity 2.5 × 10^6 cSt) was obtained from Polysciences Inc., Warrington, PA.

The silica-based ionic liquid was prepared as described previously:[4] 3.5 mL of colloidal silica (Ludox-SM, 30 wt % SiO_2, particle size: 7 nm, pH = 10) were diluted with 20 mL of deionized water. To the suspension, 5 mL of $(CH_3O)_3Si(CH_2)_3N^+(CH_3)(C_{10}H_{21})_2Cl^-$ in methanol (40%, Gelest) was added. The white precipitate formed immediately was aged for 24 h at room temperature by gently shaking it periodically. Then, the solvent was discarded and the solid was rinsed three times with water and twice with ethanol. The solid was re-suspended in ethanol, poured into a Petri dish, and dried at 70 °C. The corresponding sulfonate was prepared by treating 1 g of the chloride analogue with 15 mL of a 10% w/v solution of $R(OCH_2CH_2)_7O(CH_2)_3SO_3^-K^+$ (R: C_{13}−C_{15} alkyl chain, Aldrich) in water at 70 °C for 24 h. The solvent was discarded and the material was washed several times with water and dried at 70 °C.

Preparation of Dye-Containing Films. To prepare solutions of the dyes in the ionic liquid, known amounts of the dye and the

(4) Bourlinos, A. B.; Herrera, R. A.; Chalkias, N.; Jiang, D. D.; Zhang, Q.; Archer, L. A.; Giannelis, E. P. *Adv. Mater.* **2005**, *17* (2), 324−237.

(5) Lin, C.-T.; Böttcher, W.; Chou, M.; Creutz, C.; Sutin, N. *J. Am. Chem. Soc.* **1976**, *98* (21), 6536−6544.

ionic liquid were dissolved in a common solvent. The platinum dyes were dissolved in tetrahydrofuran (THF, 15 ppm), and the ruthenium dye was dissolved in chloroform (15 ppm). A weighed amount of ionic liquid (0.050 g) was then dissolved in 1.0 g of each solution. Each of the solutions obtained was cast onto a Corning Micro slide (No. 2947, plain, 3 in. × 1 in., thickness: 0.96−1.06 mm, cut into 0.75 in. × 1 in. pieces), which had been cleaned with THF and acetone. The slide was placed in a covered container with a small opening in order to slow the solvent evaporation rate. The container was wrapped with aluminum foil to avoid light and kept at room temperature for 24 h. The dense film that formed on the glass slide was dried at 60 °C in an oven at ambient pressure for 24 h, followed by annealing at 60 °C under vacuum (less than 1 Torr) in a vacuum oven for 48 h. After cooling to room temperature, the samples were transferred to a desiccator and stored in the dark. The final film thickness was on the order of 0.1 mm, and the bulk-averaged dye concentration was about 300 ppm (PtOEP, 330 ppm; PtTFPP, 300 ppm; PtTPP, 293 ppm; $[Ru(dpp)_3]Cl_2$, 303 ppm). Although the ionic liquid exhibits liquidlike behavior, a thin film of this liquid on a solid support like a microscope slide did not flow over several hours when it was placed vertically.

Many experiments have already been reported for the dyes listed above in PDMS and C_4PATP films. A few additional samples were prepared for these experiments as described previously,[6] in which the dye concentration was ca. 100 ppm and the film thickness was ca. 0.1 mm.

A solution of pyrene in the ionic liquid was prepared by a different method. First, we prepared a film of the ionic liquid (from THF) on a clean quartz disk (round, 1 in. diameter). The film was dried as described above and then placed in a sealed polypropylene container that also contained pyrene crystals. The container was kept at room temperature in the dark over 40 days. Sufficient pyrene evaporated and dissolved in the ionic liquid film to give a useful fluorescence signal.

Phosphorescence Emission and Phosphorescence Decay Measurement. For steady-state PL measurements, an ionic liquid film was placed in a closed vacuum/pressure chamber and fitted into the optical path of the fluorescence spectrometer. The slits for the excitation monochromator were set at 4 nm and those of the emission monochromator were 8 nm. To resolve the fine structure of pyrene emission, the emission slits were set to be 2 nm. Samples were measured in the reflectance mode with right angle detection, and the signal intensity was recorded in the S&R (signal and reference) mode in 1.0 nm steps. To ensure the linearity of response, the sample source signal was always kept to less than 2×10^5 count s^{-1}. After each change in pressure, the sample was allowed to equilibrate for 10 min before the next luminescence measurement was carried out. The air/oxygen pressure inside the chamber was controlled over a range from 0 to 1000 Torr through a combination of a vacuum pump and a compressed gas line. Gas pressure was measured by an MKS Baratron 626A 13TAE absolute pressure transducer (1000 Torr with an accuracy of ±0.25% of the reading, ±0.15% of the reading over the range of 10 to 1000 Torr). For quantitative intensity measurements, data were acquired in the time-base scan mode (fixed excitation and emission wavelengths) at one point per second, for 300 s. Then the average emission intensity was calculated from these data. This data acquisition technique improves the precision of the intensity measurements, with a typical precision of ±2% except at very high oxygen partial pressures when the residual PL intensity was very weak. A similar vacuum/pressure sample chamber was used for the pulsed laser experiments. It was equipped with an MKS Baratron 626A 12TAD absolute pressure transducer with similar specifications to that used for steady-state measurements.

Data Analysis. In fluid solution, luminescence intensities and decay times for quenching by oxygen follow the simple Stern−Volmer equation.[7]

$$\frac{I^o}{I} = \frac{\tau^o}{\tau} = 1 + k_q \tau^o [Q] \tag{1}$$

where I and τ are, respectively, the luminescence intensity and the luminescence decay lifetime, and the values superscripted with "o" refer to values in the absence of quencher. [Q] denotes the molar concentration of the quencher. When the quencher is a gas such as oxygen, the concentration in solution will be proportional to its partial pressure, p_{O_2} (Henry's law). Hence one can write

$$\frac{I^o}{I} = 1 + K_{SV} p_{O_2} \tag{2}$$

where the Stern−Volmer constant K_{SV} contains all of the proportionality constants relating the external oxygen pressure to the luminescence intensity.

Dyes in homogeneous fluid solution normally exhibit simple exponential luminescence decays. For some dyes dissolved in polymer matrixes and most dyes adsorbed to solid surfaces such as silica, the luminescence intensity decay profiles $I(t)$ are non-exponential. These decay curves can be fitted to a sum of exponential terms,

$$I(t) = \sum_i A_i \exp\left(-\frac{t}{\tau_i}\right) \tag{3}$$

where A_i are the normalized preexponential factors for the terms with lifetime τ_i and the intensity-weighted mean lifetime can be calculated from the fitting parameters as

$$\langle \tau \rangle = \sum_i A_i \tau_i \tag{4}$$

When the Stern−Volmer plots are linear, they are amenable to more sophisticated interpretation. The relevant mathematical expressions for this analysis will be presented in a later section of the paper.

Results

Properties of the Dyes in the Ionic Liquid. In this section, we examine the spectroscopic properties of a variety of dyes dissolved in the ionic liquid. With the exception of pyrene, the dyes chosen for examination are transition metal complex dyes that exhibit long-lived (microsecond) emission (phosphorescence) from excited states with triplet-like character. The structure of these dyes is shown in Chart 2. To prepare solutions of dyes in this fluid, known weights of dye and ionic liquid were dissolved in a common volatile solvent and then the mixture was cast onto a glass substrate and allowed to dry. Any remaining solvent was removed under vacuum at 60 °C. The ionic liquid is sufficiently viscous that thin films of this material on a flat substrate do not flow noticeably over short time periods (several hours) when the substrate is placed in a vertical position. This property facilitates making spectroscopic measurements with

(6) Lu, X.; Han, B.-H.; Winnik, M. A. *J. Phys. Chem. B* **2003**, *107* (48), 13349−13356.

(7) Lakowicz, J. R. *Principles of Fluorescence Spectroscopy*, 2nd ed.; Kluwer Academic/Plenum Publishers: New York, 1999.

Chart 2. Molecular Structures of the Phosphorescent Dyes Employed

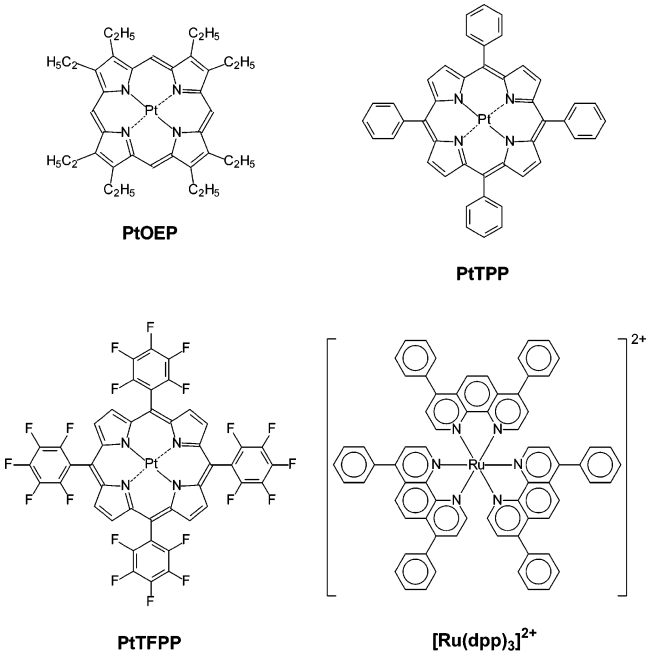

conventional instrumentation. Pyrene is too volatile for its solutions in the ionic liquid to be prepared in this way. To prepare pyrene solutions, we placed a film of ionic liquid on its substrate in a closed container containing a small amount of pyrene crystals. Over a period of 40 days at ambient temperature sufficient pyrene sublimed and dissolved in the liquid to give meaningful fluorescence spectra. The concentration of pyrene in the sample (ca. 3×10^{-4} M) was estimated by a UV absorption measurement using the extinction coefficient of pyrene in methanol and in THF as models.

Pyrene was chosen as a solute because its absorption and emission spectra are sensitive to its environment. The peak positions in the absorption spectrum are sensitive to the local polarizability, and its fluorescence spectrum reports on the local polarity of its environment. The UV−Vis absorption spectrum of pyrene in the ionic liquid is shown in Figure 1. The ionic liquid itself shows a strong absorption below 300 nm. The characteristic absorption peaks of pyrene are at 275, 322, and 338 nm and are consistent with the peaks of the corresponding excitation spectra (emission monitored at 392 nm). Thus the ionic liquid appears to be a normal solvent for pyrene. The absorption peak positions are red-shifted by about 4 nm from the corresponding peak positions for pyrene in methanol and 2 nm from those of pyrene in THF,[8] indicating that the pyrene molecules are located in an environment somewhat more polarizable than either solvent.

The pyrene emission spectrum ($\lambda_{ex} = 338$ nm) is shown in Figure 2. At this pyrene concentration, we see peaks only from monomer emission, and no excimer can be detected. The first peak in its fluorescence spectrum (the (0,0) band) is due to a symmetry-forbidden transition, and its intensity is enhanced by a polar environment, relative to that of the third peak in the spectrum. This I_1/I_3 intensity ratio is a very useful measure of solvent polarity,[9] and for microheterogeneous systems such as micelles or vesicles provides a measure of the local polarity of the pyrene environment.[10] In the spectrum in Figure 2, $I_1/I_3 = 1.3$, suggesting a rather polar environment for the pyrene molecules. This value can be compared to values of 1.87 for water and 0.58 for hexane, and also to a value of 1.35 in methanol, 1.37 in acetic acid, 1.25 in chloroform, and 1.35 in THF. Based on the absorption and emission spectra of pyrene, we conclude that the pyrene is located in an environment somewhat less polar and more polarizable than that of a THF solution.

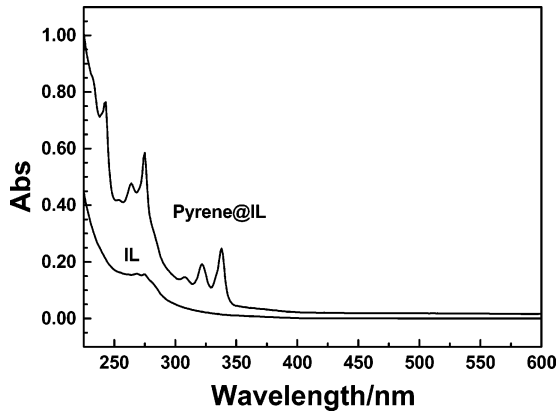

Figure 1. UV−Vis absorption spectrum of pyrene in the soft-sphere ionic liquid film (Pyrene@IL) and the absorption spectrum of the ionic liquid itself (IL).

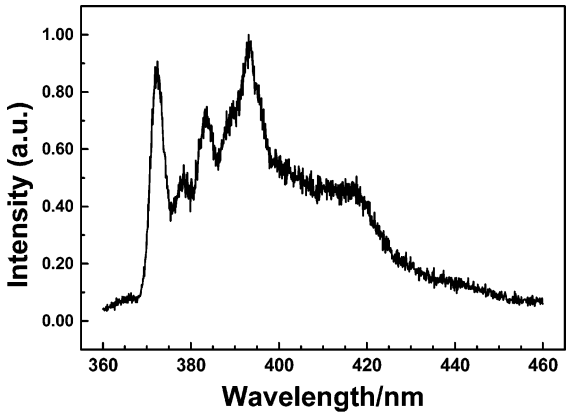

Figure 2. The emission spectrum of pyrene in the soft-sphere ionic liquid film.

The emission and excitation spectra of PtOEP (330 ppm) dissolved in the ionic liquid film are shown in Figure 3A. These spectra are typical for solutions of this dye, with the strong absorbance of the Soret band appearing at 383 nm, and the two bands at 536 and 500 nm due to the $^1S_0 \rightarrow {}^1S_1$ (π,π^*) transition. The emission appears as expected as a sharp peak centered at 645 nm. The excitation spectra of PtTFPP and PtTPP in the ionic liquid resemble those of PtOEP, but the band positions of PtTFPP and PtTPP are bathochromically shifted by a few nanometers. The emission spectra are similar in shape, with the peak position at 650 nm for PtTFPP and 663 nm for PtTPP. To put these results

(8) λ_{max} values for pyrene in THF (274, 320, and 336 nm) and in methanol (272, 318, and 334 nm).

(9) Dong, D. C.; Winnik, M. A. *Photochem. Photobiol.* **1982**, *35* (1), 17−21.
(10) Kalyanasundaram, K.; Thomas, J. K. *J. Am. Chem. Soc.* **1977**, *99* (7), 2039−2044.

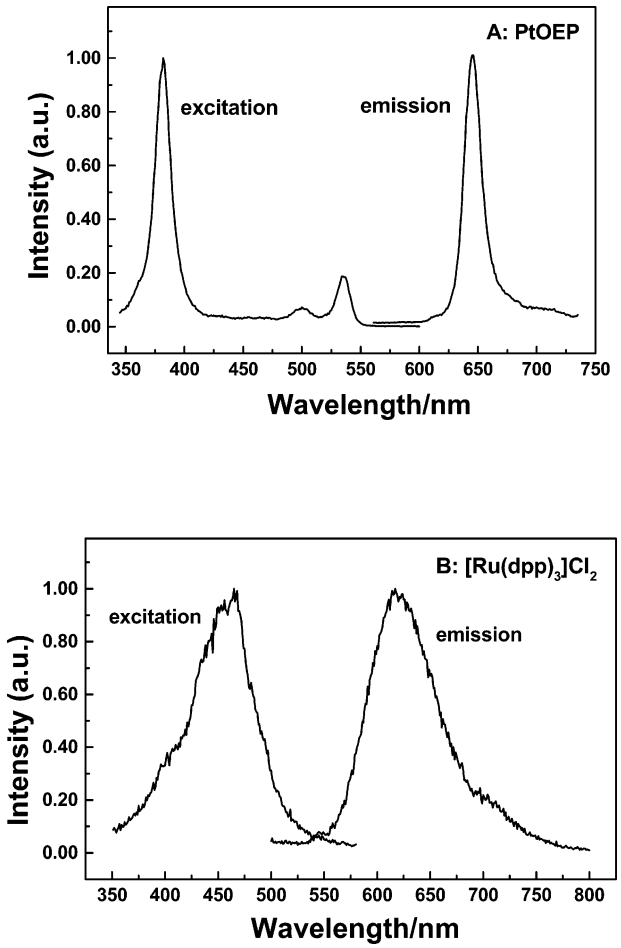

Figure 3. The emission and excitation spectra of PtOEP (A) and [Ru(dpp)$_3$]Cl$_2$ (B) in the soft-sphere ionic liquid film.

Table 1. Excitation, Emission Peak Positions, and Unquenched Average Lifetime of Various Dyes in the Ionic Liquid Film

	$\lambda_{ex.max}$ (nm)	$\lambda_{em.max}$ (nm)	τ^o (μs)	$\lambda_{ex.max}$ (nm)[a]	$\lambda_{em.max}$ (nm)[a]
PtOEP	383	645	66.0	383	645
PtTFPP	393	650	21.7[b]	392	649
PtTPP	398	663	54.2		
[Ru(dpp)$_3$]Cl$_2$	462	618	5.7	~460	605

[a] In C_4PATP, see ref 6. [b] The unquenched average lifetime $\langle\tau\rangle^o$.

in context, we present each of the peak wavelengths in Table 1 and for comparison provide the peak wavelengths for the dyes dissolved in the polymer poly(*n*-butylthionyl phosphazene) (C_4PATP).[6] It is evident that the excitation and emission peak positions for PtOEP and PtTFPP in C_4PATP polymer and in the silica nanoparticle-based ionic liquid film are almost the same, indicating the environments for the dyes are similar. The emission and excitation spectra of [Ru(dpp)$_3$]Cl$_2$ (303 ppm) dissolved in the ionic liquid film are shown in Figure 3B. The excitation spectrum shows a broad peak between 400 and 500 nm, which is very similar to that in the C_4PATP polymer. However, the emission peak is at 618 nm, which is at a longer wavelength than that in C_4PATP (Table 1).

The phosphorescence decay profiles for PtOEP and PtTPP in the ionic liquid film in the absence of oxygen are exponential with unquenched lifetimes (τ^o) of 66.0 and 54.2 μs, respectively. The corresponding decay profile for PtTFPP (300 ppm) in the ionic liquid is nonexponential in the absence of oxygen and is easily fitted to a sum of two exponential terms, giving an unquenched average (mean) lifetime $\langle\tau^o\rangle$ of 21.7 μs. A somewhat surprising finding is that the decay profile for [Ru(dpp)$_3$]Cl$_2$ (303 ppm) in the ionic liquid can also be well-fitted to a simple exponential function (with τ^o = 5.7 μs). While the decay profile for this dye and other ionic ruthenium dyes are exponential in fluid media where solvent relaxation is rapid on the time scale of the excited state lifetime, the decay profile is strongly nonexponential in polymer media such as C_4PATP.

Table 2. Comparison of Various Dyes in Two Polymer Films, PDMS and C_4PATP, and the Ionic Liquid Film

	ionic liquid		C_4PATP[a]		PDMS	
	lifetime (μs)	K_{sv} (Torr^{-1})	lifetime (μs)	K_{sv} (Torr^{-1})	lifetime (μs)	K_{sv} (Torr^{-1})
PtOEP	66.0	0.32	102	0.39	65[b]	1.38
PtTFPP	21.7	0.076	66	0.17	33.3	0.38
PtTPP	54.2	0.18				
[Ru(dpp)$_3$]Cl$_2$	5.7	0.0084	6.2	0.013		

[a] Reference 6. [b] Reference 11.

These lifetimes of the dyes examined are presented in Table 2, and compared to the corresponding lifetimes for the dyes, where available, in two polymeric media, poly(dimethylsiloxane) (PDMS) and C_4PATP. One sees that, for PtOEP and PtTFPP, the τ^o values in the ionic liquid are comparable to those in PDMS, but significantly shorter than those in C_4PATP. [Ru(dpp)$_3$]Cl$_2$ is insoluble in PDMS, a nonpolar medium. In C_4PATP, it has a nonexponential decay in the absence of O_2, with a mean lifetime $\langle\tau^o\rangle$ very close to the (exponential) lifetime determined for this dye in the ionic liquid.

Luminescence Quenching Experiments. When the dye-containing films described above were placed in a chamber and equilibrated with a certain partial pressure of oxygen, p_{O_2}, the PL intensity was reduced. As p_{O_2} was increased, the PL intensity decreased due to more extensive oxygen quenching of the excited state. The emission peak at 645 nm for PtOEP in the ionic liquid decreases in intensity but does not shift or change in shape over the entire pressure range. This phenomenon is typical for all the dyes investigated here. If there were dyes in different environments with different susceptibility to oxygen quenching, one might observe a spectral shift at high oxygen pressures, where the emission would be dominated by the dyes that were most difficult to quench.

Intensity Stern−Volmer plots for the four dyes examined in the ionic liquid are presented in Figure 4. The plot focuses on I^o/I values up to 12, which corresponds to quenching of >90% of the emission intensity. The plots are linear over the entire pressure range for PtOEP and PtTPP, whereas the data for PtTFPP show a downward curvature. While the plot appears linear for [Ru(dpp)$_3$]Cl$_2$, the data also show a slight downward curvature at higher oxygen pressures (in the range of 400−700 Torr). For these dyes, the Stern−Volmer constants are calculated from the linear portion of the plot in the low oxygen pressure range. The K_{SV} values are listed in Table 3. A general feature of these data is that the slopes increase in the order of the τ^o values of each dye. This is consistent with the simple prediction of eq 1. If the

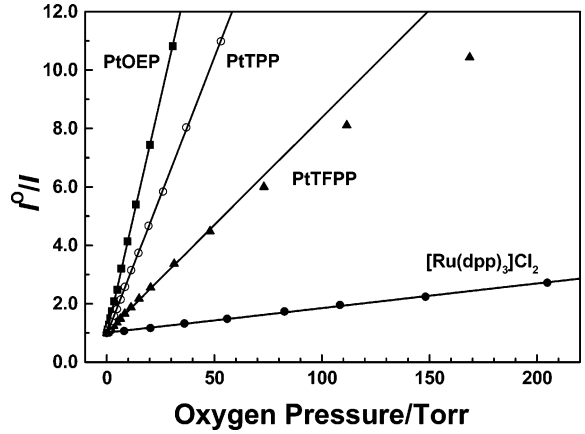

Figure 4. The intensity Stern−Volmer plots for different dyes in the soft-sphere ionic liquid film: PtOEP, solid square; PtTPP, open circle; PtTFPP, solid triangle; $[Ru(dpp)_3]Cl_2$, solid circle.

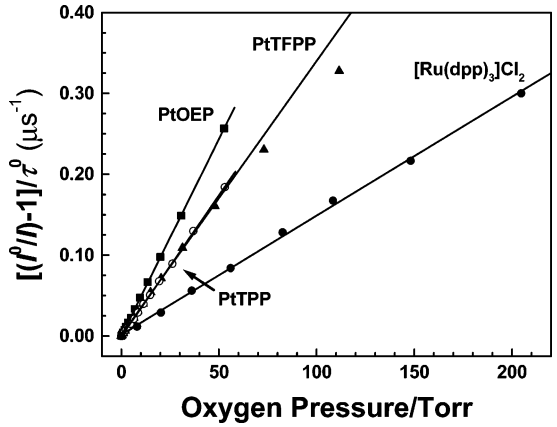

Figure 5. Modified intensity Stern−Volmer plots $\{[(I^o/I) - 1]/\tau^o$ vs $p_{O_2}\}$ for different dyes in the soft-sphere ionic liquid film: PtOEP, solid squares; PtTPP, open circles; PtTFPP, solid triangles; $[Ru(dpp)_3]Cl_2$, solid circles.

Table 3. Stern−Volmer Constants for Various Dyes in the Ionic Liquid Film from Intensity and Decay Profile Measurement

	intensity measurement			lifetime measurement		
	r	K_{sv} ($Torr^{-1}$)	intercept	r	K_{sv} ($Torr^{-1}$)	intercept
PtOEP	1.0000	0.32	0.989	0.9994	0.27	0.995
PtTFPP	0.9995	0.074	1.021	0.9984	0.060	1.009
PtTPP	0.9999	0.19	0.958	0.9984	0.098	0.981
$[Ru(dpp)_3]Cl_2$	0.9994	0.0084	1.010	0.9994	0.011	1.003

unquenched lifetime were the only important factor, replotting the data as $(1/\tau^o)[(I^o/I) - 1]$ vs p_{O_2} would reduce all of the data to a common line. As the plot in Figure 5 indicates, there is a reduction in the discrepancies between the plots, but differences remain.

PL decay measurements provide another measure of the susceptibility of the dyes to oxygen quenching. Decay profiles for each dye at a series of oxygen partial pressures are presented in Figure S1 in the Supporting Information. A common feature of these decay traces is that there is an enhancement in curvature in the semilogarithmic plots at elevated oxygen pressure. For PtOEP and $[Ru(dpp)_3]Cl_2$, the decays are nearly exponential, and the curvature appears only as a weak tail. For PtTPP, the decays are exponential at low oxygen pressures but become more curved as this pressure is increased. For PtTFPP, the decays are nonexponential over the entire range of pressures. Nonexponential decays at finite

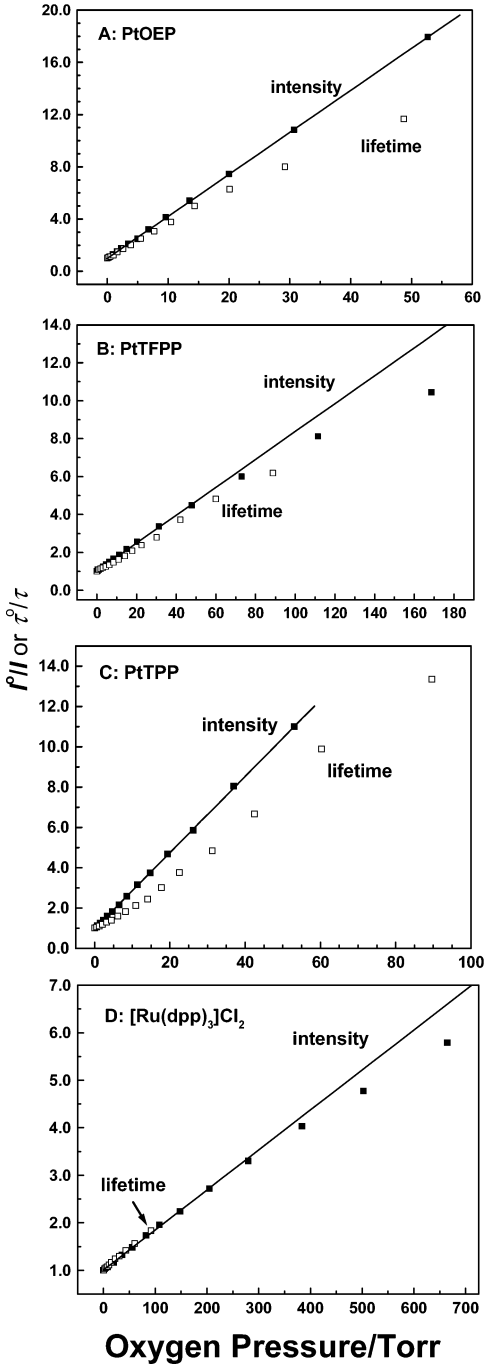

Figure 6. The intensity and lifetime Stern−Volmer plots of PtOEP (A), PtTFPP (B), PtTPP (C), and $[Ru(dpp)_3]Cl_2$ (D) in the soft-sphere ionic liquid film.

oxygen pressure are an indication that the dyes are distributed over a range of different environments, either with different intrinsic lifetimes or different oxygen diffusivities.[12]

In Figure 6 we present lifetime Stern−Volmer plots of the data in Figure S1. Thus, these Stern−Volmer plots were constructed with values of $\langle\tau^o\rangle/\langle\tau\rangle$ for PtTFPP and $\tau^o/\langle\tau\rangle$ for the other three dyes. The lifetime SV plots for $[Ru(dpp)_3]Cl_2$ and PtTFPP are linear for the pressures examined and closely track that for the intensity data. For PtOEP, the lifetime SV plot is linear and tracks that for the intensity

(11) Lu, X.; Manners, I.; Winnik, M. A. *Macromolecules* **2001**, *34* (6), 1917−1927.
(12) Hartman, P.; Trettnak, W. *Anal. Chem.* **1996**, *68* (15), 2615−2620.

data up to $\tau^o/\langle\tau\rangle \approx 5$, but then begins to deviate from the intensity data and curves downward. For PtTPP, the lifetime SV plot is rather unusual, showing an upward curvature that is very difficult to explain. K_{SV} values were calculated from the slopes of the SV plots in the low-pressure regime. These values are presented in Table 3.

Discussion

According to eq 1, for PL quenching in homogeneous fluid media one expects superimposed lines for the plots of I^o/I and τ^o/τ against quencher concentration. For these types of systems, one sometimes observes linear plots of τ^o/τ vs [Q], but an upward curvature of the I^o/I plot at elevated quencher concentrations. This type of behavior is easy to explain in terms of two competing quenching processes, *dynamic quenching* which involves dye and quencher diffusion following dye excitation, and *static quenching*. In the latter process, some dye molecules are so close to quenchers that they are quenched instantaneously after photoexcitation. Thus, these dyes do not contribute to the measured lifetime, but they do contribute to the decrease in luminescence intensity.

In the experiments reported here, O_2 is the quencher. While the molar concentration of O_2 in the ionic liquid is not known, we expect, based on Henry's law, that $[O_2]$ will be proportional to p_{O_2}. When we examine the data in Figure 6, we find that for $[Ru(dpp)_3]Cl_2$ and $p_{O_2} < 60$ Torr ($I^o/I < 1.5$) that the two plots can be fitted by the same line. We find a similar situation for PtOEP for $p_{O_2} < 10$ Torr ($I^o/I < 3$). For PtTFPP, the intensity and lifetime data are very similar, but only at low extents of quenching ($I^o/I < 1.5$). Here we have less confidence in the data because, even at these low oxygen pressures, the dye decay is not exponential, suggesting that the dyes are in a distribution of environments with different lifetimes. At higher oxygen pressures, deviations are found. In this range of pressures, for the three Pt dyes, the τ^o/τ plots lie below the I^o/I plots, suggesting that static quenching plays a role in these experiments. What is unusual about these experiments is that the intensity plots are linear over the entire range of pressures, whereas the lifetime plots show deviations. Carraway et al. described the kinetics of oxygen quenching of $[Ru(bpy)_3]^{2+}$ (bpy = bipyridyl) adsorbed on porous silica disks.[13] Here the intensity Stern−Volmer plot exhibited a smaller curvature than the mean lifetime Stern−Volmer plot. We have seen this type of phenomenon previously in the case of silica nanoparticles dispersed in polymer matrixes such as PDMS.[11] It is tempting to associate this phenomenon with either dye adsorption or oxygen adsorption onto the silica nanoparticles present in the system.

Quenching and Oxygen Permeability in the Medium. The permeability P of a medium to a gas is the product of its diffusion coefficient D times its solubility S, where S is the proportionality constant (Henry's law constant) between the partial pressure of the gas and its molar concentration in the medium. For dyes dissolved in polymers films, a Stern−Volmer analysis of oxygen quenching data allows one to calculate the permeability of the polymer to oxygen. This connection arises in the following way: Luminescence quenching by oxygen is a diffusion-controlled process. Thus, the second-order quenching rate constant k_q (see eq 1) can be set equal to the diffusion-controlled rate constant k_{diff}. According to the theory of diffusion-controlled reactions,

$$k_{diff} = 4\pi\alpha R_{eff} N_A D_m \tag{5}$$

where N_A is Avogadro's number and D_m is the mutual diffusion of the dye and the quencher ($D_m = D_{dye} + D_{O_2}$). Since the dye molecules are much larger and less mobile than the oxygen molecules in the medium, one can to a good approximation set $D_m = D_{O_2}$. R_{eff} is the characteristic encounter radius of the dye, and α describes the fraction of dye-quencher encounters that result in quenching. In principle, the value of α for oxygen quenching of triplet states is 1/9 since that is the fraction of random encounters between triplet oxygen and the dye triplet that lead to the dye in its singlet ground state. In reality, for dense systems, multiple collisions between the dye and the quencher within a solvent cage increase the quenching probability per diffusive encounter. The lifetime of the encounter pair increases as D_m decreases. Within the context of this model, if one can vary D_m (i.e., by varying viscosity through a change in temperature), then in the limit of $D_m \rightarrow 0$, $\alpha \rightarrow 1$, R_{eff} approaches the true encounter radius. In actual practice, it is more common to assume a value for αR_{eff} and use this value for further analysis of the data.

Since $[O_2] = S_{O_2} p_{O_2}$, and the oxygen permeability $P_{O_2} = D_{O_2} S_{O_2}$, eq 1 can be rewritten as

$$\frac{1}{\tau^o}\left(\frac{I^o}{I} - 1\right) = 4\pi\alpha R_{eff} N_A p_{O_2} p_{O_2} \tag{6}$$

With this expression, the slopes of the Stern−Volmer plots can be interpreted in terms of the oxygen permeability of the medium if a reasonable approximation for αR_{eff} can be made. We have previously reported oxygen-quenching experiments for PtOEP in PDMS and C_4PATP polymer films. We could obtain reasonable values for P_{O_2} in these media with the assumption that $\alpha R_{eff} = 1.0$ nm. For films of $[Ru(dpp)_3]Cl_2$ in C_4PATP, the slope was smaller. Since P_{O_2} is a property of the medium and not the dye, these results could be understood only if αR_{eff} were smaller (0.50 nm) for the ruthenium dye.[6]

To pursue this analysis, we treat the quenching of PtOEP and $[Ru(dpp)_3]Cl_2$ as "normal" since the PL decay profiles are exponential at low values of p_{O_2}, and use the data in the pressure range where the I^o/I and τ^o/τ plots overlap. From eq 4, assuming a value of $\alpha R_{eff} = 1.0$ nm for PtOEP, we calculate $P_{O_2} = 4 \times 10^{-12}$ mol cm^{-1} s^{-1} atm^{-1}. The same analysis gave an apparent P_{O_2} value from the ruthenium dye which is about one-third the magnitude obtained from the PtOEP data. As we stated in the previous paragraph, oxygen permeability is a property of the medium, and the two data sets can be reconciled if $\alpha R_{eff} = 0.30$ nm for $[Ru(dpp)_3]Cl_2$. It is satisfying to see that PtOEP and $[Ru(dpp)_3]Cl_2$ behave in a similar way in the ionic liquid and in the polar aprotic

(13) Carraway, E. R.; Demas, J. N.; DeGraff, B. A. *Langmuir* **1991**, *7* (12), 2991−2998.

C_4PATP matrix, even if the value of αR_{eff} deduced for the ruthenium dye in the ionic liquid is somewhat smaller than that in the polymer film.

A Heterogeneous Medium. The ionic liquid consists of cells derived from soft spheres consisting of a hard silica core surrounded by a corona of flexible chains that represent about 90 vol % of the dense medium. The corona itself is heterogeneous, consisting of an ionic shell separated from the silica surface by a three-carbon spacer. Outside of this layer is the external phase consisting of both PEG chains and alkyl tails. Strong Coulombic and ion-pair interactions ensure that the $-OSO_3^-$ groups of the alkyl PEG sulfate are in close proximity to the tetraalkylammonium groups covalently attached by the short space to the silica surface.

Dyes dissolved in this medium seek their own preferred environment. From the I_1/I_3 ratio of pyrene emission, we learn that pyrene prefers a polyether-like environment contributed by the PEG chains. None of the dyes behave as though they were strongly adsorbed to the silica nanospheres. For example, we have shown that, in PDMS containing silica nanoparticles treated to render them dispersible in organic media, the absorption and emission spectra of PtOEP are strongly perturbed over that in PDMS itself, indicating that the dye is strongly adsorbed to the silica particles. Under these conditions, its PL decay profile is strongly nonexponential. In contrast, the excitation and emission spectra of PtOEP in C_4PATP containing the same silica nanoparticles are nearly unaffected, and the decay profile remains exponential. The polar aprotic medium is a much better solvent for the dye, and the dye prefers to remain in the fluid medium. In this sense, PtOEP in the ionic liquid resembles that in C_4PATP, suggesting that it resides in PEG-rich domains of the fluid.

The nonexponential decay of PtTFPP, even in the absence of oxygen, suggests that this dye is distributed among domains that impart a different characteristic lifetime to the decay. We observe no substantial band broadening in the PL spectrum that would suggest dye aggregation accompanying extensive adsorption to silica. In contrast, the results for PtTPP are difficult to understand. The luminescence decays are largely exponential, not only in the absence of oxygen but even at modest oxygen pressure. In this respect, this dye resembles PtOEP. On the other hand, both the intensity and the lifetime Stern−Volmer plots for this dye exhibit an upward curvature. While one can discern this curvature by eye in the data in Figures 5 and 6, another clearer indication of the curvature is the magnitude of the intercept to a linear fit through these data. As one can see in Table 3, the other 3 dyes have intercepts very close to 1.0 for both the intensity and the lifetime Stern−Volmer plots, whereas for PtTPP, the intercepts are significantly smaller.

Perhaps the most interesting aspect of the lifetime measurements is the nature of the data obtained for $[Ru(dpp)_3]Cl_2$. Its PL decays can be fitted rather well to a single-exponential term over the entire range of oxygen pressures. In solution in low-viscosity solvents, this dye exhibits an exponential decay over a wide range of quencher concentrations. Solvent relaxation is rapid, and all the dyes experience the same average environment during their lifetime. In polymeric media such as C_4PATP, ionic dyes commonly exhibit nonexponential decays. We often attribute this observation to a combination of two factors, slow relaxation processes in the medium coupled with a distribution of counterion arrangements around each dye. In the ionic liquid, the $[Ru(dpp)_3]^{2+}$ cation can interact with the surfactant-like $R-EO_x-OSO_3^-$ component of the solvent. We imagine that the dye is selectively dissolved in the ionic corona that surrounds each of the dense silica cores, and that all of the dyes experience a similar microenvironment. This environment is different from that probed by PtOEP or pyrene.

We have to keep in mind that another consequence of the heterogeneous nature of the ionic fluid may be that the concentration and diffusivity of oxygen are different in the various microdomains. The low value of αR_{eff} deduced for the ruthenium dye in the ionic liquid may be a consequence of assuming that P_{O_2} is everywhere uniform. If, in contrast, we assume that αR_{eff} is an intrinsic property of the dye, we could then infer that P_{O_2} is lower in the ionic domains surrounding the silica nanoparticles than it is in the hydrocarbon and PEG-rich fluid regions between the core particles.

Summary

We examined the photoluminescent properties of a series of phosphorescent dyes dissolved in a core−shell "soft-sphere" ionic liquid matrix consisting of a 7 nm diameter silica core surrounded by a mobile phase consisting of end-grafted flexible chains. While this medium is macroscopically uniform in composition, it is locally heterogeneous on the nanometer length scale. Luminescent dyes provide an opportunity for assessing some of the properties of this local heterogeneity.

The dyes employed were platinum porphyrin complexes (PtOEP, PtTPP, and PtTFPP) and a ruthenium tris-phenanthroline complex ($[Ru(dpp)_3]Cl_2$). None of the dyes exhibited strong spectral shifts that would be anticipated if the dyes had adsorbed strongly to the silica nanoparticles present within each cell of the fluid. Other evidence indicated that some of the dyes (e.g., $[Ru(dpp)_3]Cl_2$) were localized selectively within individual domains in the fluid phase, and the nonexponential PL decays of PtTFPP, even in the absence of oxygen, suggest that this dye is located in a distribution of different environments characterized by different intrinsic PL lifetimes.

The phosphorescence-quenching behavior of these dyes was investigated through monitoring the changes in phosphorescence emission intensity and lifetime upon varying the external oxygen pressure. At low to modest oxygen partial pressures, the intensity and lifetime Stern−Volmer plots were superimposable and linear. The sole exception was PtTPP, in which both plots exhibited an unusual upward curvature that is very difficult to explain. The PL decay profiles of both PtOEP and $[Ru(dpp)_3]Cl_2$ could be fitted to a simple exponential form over a range of partial oxygen pressures. Taking the behavior of PtOEP as "normal", we calculate an oxygen permeability in the liquid of $P_{O_2} = 4 \times 10^{-12}$ mol cm^{-1} s^{-1} atm^{-1}, comparable to that of C_4PATP ($3.9 \pm 0.4 \times 10^{-12}$ mol cm^{-1} s^{-1} atm^{-1}) but smaller than that ($18 \pm 2 \times 10^{-12}$ mol cm^{-1} s^{-1} atm^{-1}) for the high

oxygen permeability polymer PDMS.[12] The smaller slope of the Stern−Volmer quenching plot for $[Ru(dpp)_3]Cl_2$ could be rationalized in terms of two factors, the known smaller cross section for quenching by oxygen for this dye coupled with the likelihood that this dye is located in a more rigid ionic environment characterized by a somewhat smaller local diffusion coefficent for oxygen.

Acknowledgment. The Toronto authors thank NSERC Canada and the Province of Ontario, through their ORDFC program, for their support of this research. The Cornell authors gratefully acknowledge the support by AFOSR, the Cornell Center for Materials Research (CCMR) and ONR.

Supporting Information Available: The phosphorescence decay profiles of PtOEP, PtTFPP, PtTPP, and $[Ru(dpp)_3]Cl_2$ in the soft-sphere ionic liquid film at various oxygen pressures (PDF). This material is available free of charge via the Internet at http://pubs.acs.org.

CM050553E